The Open Chemical Engineering Journal
ISSN: 1874-1231
DOI: 10.2174/0118741231367952250224071438, 2025, 19, e18741231367952

RESEARCH ARTICLE **OPEN ACCESS**

$KCo_{1/2}Hf_{1/2}(MoO_4)_2$ – A Novel Glaserite-like Molybdate Exhibiting Two-dimensional Negative Thermal Expansion

Evgeniy Kovtunets[1,*], Tatyana S. Spiridonova[1], Yunna L. Tushinova[1], Tsyrendyzhit T. Bazarova[1], Alexandra V. Logvinova[1] and Bair G. Bazarov[1]

[1] *Laboratory of Oxide Systems, Baikal Institute of Nature Management, Siberian branch of the Russian Academy of Sciences, Ulan-Ude 670047, Russia*

Abstract:

Introduction: Due to the peculiarities of the crystal structure and composition, complex molybdates exhibit valuable functional properties. Although the intensive search for NTE materials has been going on for many years, the investigation of the mechanisms and structure-property relationships causing the "thermal shrinkage" effect is still relevant. Here, we report on the 2D-NTE effect in a new ternary molybdate $KCo_{1/2}Hf_{1/2}(MoO_4)_2$ with a layered glaserite-like structure, and its thermal deformations and ionic conductivity were investigated.

Methods: The $KCo_{1/2}Hf_{1/2}(MoO_4)_2$ was synthesized through the ceramic method. HT-PXRD patterns were acquired using a Bruker D8 ADVANCE diffractometer and subsequently utilized for Rietveld analysis. Structure refinement and lattice parameter calculations were conducted with TOPAS 4.2, while calculation of the thermal expansion tensor and visualization were carried out in the TTT. ATR-IR spectroscopy was used to characterize the coordination of the molybdenum atoms. TG and DSC analyses were performed using an STA 449 F1 Jupiter thermal analyzer. Electrical conductivity was assessed using a Z-1500J impedance meter using the two-contact impedance spectroscopy method.

Results: $KCo_{1/2}Hf_{1/2}(MoO_4)_2$ crystallizes with the trigonal glaserite-type structure in space group $P3\text{-}m1$ with unit cell parameters of a = 5.76190 (3), c = 7.14788 (5) Å, V = 205.51 (1) Å^3, and Z = 1. DSC indicated that $KCo_{1/2}Hf_{1/2}(MoO_4)_2$ melted at 699°C with decomposition. The observed 2D negative thermal expansion in the *ab* plane did not lead to a reduction in the cell volume. The studied ternary molybdate $KCo_{1/2}Hf_{1/2}(MoO_4)_2$ ($\alpha_V = 148\times10^{-6}$ °C^{-1} at 600°C) can be categorized as a high-expansion material.

Conclusion: $KCo_{1/2}Hf_{1/2}(MoO_4)_2$ has been categorized as a high-expansion material (αV = 148 × 10− 6 ◦C− 1 at 600◦C). At higher temperatures, the compound demonstrated notable ionic conductivity, values up to 0.42·10^{-3} S/cm (570°C) at E_a = 0.8 eV.

Keywords: Ternary molybdate, Solid-phase synthesis, Thermal expansion, Conductivity, Luminescent, HT-PXRD.

Received: November 11, 2024
Revised: January 10, 2025
Accepted: January 15, 2025
Published: February 28, 2025

---

*Address correspondence to this author at the Laboratory of Oxide Systems, Baikal Institute of Nature Management, Siberian branch of the Russian Academy of sciences, Ulan-Ude670047, Russia; Phone: +7 (3012) 433676; E-mail: kovtunets@gmail.com

Cite as: Kovtunets E, Spiridonova T, Tushinova Y, Bazarova T, Logvinova A, Bazarov B. $KCo_{1/2}Hf_{1/2}(MoO_4)_2$ – A Novel Glaserite-like Molybdate Exhibiting Two-dimensional Negative Thermal Expansion. Open Chem Eng J, 2025; 19: e18741231367952. http://dx.doi.org/10.2174/0118741231367952250224071438

1. INTRODUCTION

Due to the peculiarities of the crystal structure and composition, complex molybdates and tungstates exhibit valuable functional properties, including ion-conducting [1-4], magnetic [5], ferroelectric [6], photocatalytic [7], laser [8], luminescent [9-12] and others [13-15]. Compounds with negative thermal expansion (NTE), which have the capability to contract along specific directions with increasing temperature, also attract much attention. They are used to compensate for the total thermal expansion of functional materials operating under extreme conditions.

Representatives of well-known structural families with different mechanisms are used as NTE materials [16-20]. It is known that compounds with a layered structure have high structural anisotropy and, in some cases, can exhibit two-dimensional (2D) NTE behavior [21-24]. Although the intensive search for NTE materials has been going on for many years, the investigation of the mechanisms and structure-property relationships causing the "thermal shrinkage" effect is still relevant [25-27]. Here, we report on the 2D-NTE effect in a new ternary molybdate $KCo_{1/2}Hf_{1/2}(MoO_4)_2$ with a layered glaserite-like structure, and its thermal deformations and ionic conductivity were investigated.

2. METHOD

2.1. Sample Preparation

The glaserite-like ternary molybdate $KCo_{1/2}Hf_{1/2}(MoO_4)_2$ was synthesized through the ceramic method using stoichiometric quantities of K_2MoO_4 (chemically pure, Krasny Khimik Ltd., Russia) and pre-synthesized molybdates CoMoO4, Hf(MoO4)2. Stepwise annealing of the simple molybdate mixture was carried out in a muffle furnace at 450–580 °C for 150 h. Hafnium molybdate $Hf(MoO_4)_2$ was prepared from a stoichiometric mixture of HfO_2 (chemically pure, IGIC RAS, Russia) and MoO_3 heated at 350-750°C for 100 h. The simple molybdate $CoMoO_4$ was synthesized using a stoichiometric mixture of CoO (chemically pure, Krasny Khimik Ltd., Russia) and MoO_3, subjected to heating at 350–600 °C for 100 hours. The initial reagents were thoroughly mixed and ground in an agate mortar. Following each heating cycle, the samples were ground again and analyzed using XRD.

2.2. Variable Temperature Powder X-ray Diffraction

X-ray powder diffraction data for $KCo_{1/2}Hf_{1/2}(MoO_4)_2$ were acquired at room temperature using a Bruker D8 ADVANCE diffractometer (VANTEC detector, CuKα radiation) and subsequently utilized for Rietveld analysis. Scanning was performed over a range of 5 and 100° with a step of 0.02° and a speed of 0.1 s^{-1}. High-temperature powder X-ray diffraction (HT-PXRD) measurements were conducted in an Anton Paar HTK16 high-temperature chamber over a range of 30–600 °C with 50 °C increments. Structure refinement and lattice parameter calculations were conducted with the TOPAS 4.2 software [28], while calculations of the thermal expansion tensor and visualization were carried out in the TTT software package [29].

2.3. ATR-IR Spectrum

Attenuated total reflectance infrared spectroscopy (ATR-IR) was used to characterize the coordination of the molybdenum atoms. ATR-IR spectra were acquired using a SIMEX FT-801 FT-IR spectrometer equipped with a diamond ATR cell at room temperature within the range 500–1100 cm^{-1} with a resolution of 1 cm^{-1}.

2.4. Thermal Analysis

Thermogravimetric (TG) and differential scanning calorimetric (DSC) analyses were conducted using an STA 449 F1 Jupiter thermal analyzer (NETZSCH). Thermal analysis was performed in platinum crucibles across a temperature range of 30–750°C under an argon atmosphere, with a heating rate set to 10°C/min. The temperature was measured with an accuracy of ±1° using a Pt-PtRh thermocouple. Before the experiments, the blank measurement was made with an empty crucible to register the drift correction.

2.5. Impedance Spectroscopy

To study ion transport in $KCo_{1/2}Hf_{1/2}(MoO_4)_2$, its ceramic sample in the form of disk-shaped pellets (d=10 mm, h=1.9 mm) was used. Ceramic disks for electrophysical studies were prepared by pressing powder at a pressure of 1 kbar. The platinum electrodes were deposited on the flat surfaces of the pellets. For this purpose, a method of precipitation of colloidal platinum on large surfaces of tablets was used, followed by annealing for an hour at a temperature of about 600°C. Electrical conductivity was assessed using a Z-1500J impedance meter over a temperature range of 100–570°C using the two-contact impedance spectroscopy method in both heating and cooling modes (2°C/min, frequency range of 1–10^6 Hz).

3. RESULTS AND DISCUSSIONS

3.1. Rietveld Refinement

The refined lattice parameters for obtained $KCo_{1/2}Hf_{1/2}(MoO_4)_2$ are shown in Table **1**, main interatomic distances – in Table **2**, the atomic coordinates and isotropic displacement parameters – in Table **3**. The data are in good agreement with those published earlier for $KMg_{1/2}Zr_{1/2}(MoO_4)_2$ [30]. The parameters and, accordingly, the volumes of the unit cells decrease consistently (see Table **1**).

(Fig. **1**) presents the calculated and experimental XRD curves, along with the corresponding difference curve.

Table 1. Main parameters of processing and refinement of the $KCo_{1/2}Hf_{1/2}(MoO_4)_2$ and $KMg_{1/2}Zr_{1/2}(MoO_4)_2$ samples.

Compound	$KCo_{1/2}Hf_{1/2}(MoO_4)_2$	$KMg_{1/2}Zr_{1/2}(MoO_4)_2$/Refs.
Sp.gr.	**Trigonal, *P*3-*m*1**	
$R(M^{2+})$ Å, C.N. = 6	0.79 [31]	0.86 [31]
a, Å	5.76190 (3)	5.7679 (1) [30]
c, Å	7.14788 (5)	7.1744 (1) [30]
V, Å^3	205.51 (1)	206.70 (1) [30]

(Table 1) contd.....

Compound	**$KCo_{1/2}Hf_{1/2}(MoO_4)_2$**	**$KMg_{1/2}Zr_{1/2}(MoO_4)_2$/Refs.**
Z	1	1
2θ-interval, °	5–100	
R_{wp}, %	2.901	
R_p, %	2.134	
R_{exp}, %	1.134	
χ^2	2.559	
R_B, %	1.991	

Table 2. Geometric parameters (Å,º) of $KCo_{1/2}Hf_{1/2}(MoO_4)_2$.

MoO_4 - tetrahedron		**$(Co/Hf)O_6$ - octahedron**	
Bond	d	Bond	d
Mo—O(1)	1.684 (7)	(Co/Hf)—O(2)	2.138 (4) x6
Mo—O(2)	1.691 (5) x3		
(Mo—O)	1.689		
KO_{12} - icosahedron			
K—O(1)	3.3277 (2) x6	K—O(2)	2.881 (4) x6

Table 3. Fractional atomic coordinates and isotropic displacement parameters ($Å^2$) of $KCo_{1/2}Hf_{1/2}(MoO_4)_2$.

Atom	***x***	***y***	***z***	**Occ.**	**B_{iso}**
Hf	0	0	0	0.5	0.86 (10)
Co	0	0	0	0.5	0.86 (10)
K	0	0	1/2	1	1.19 (15)
Mo	1/3	2/3	0.2524 (3)	1	0.72 (6)
O1	1/3	2/3	0.488 (1)	1	0.84 (13)
O2	0.1727 (4)	0.3455 (9)	0.1770 (5)	1	0.84 (13)

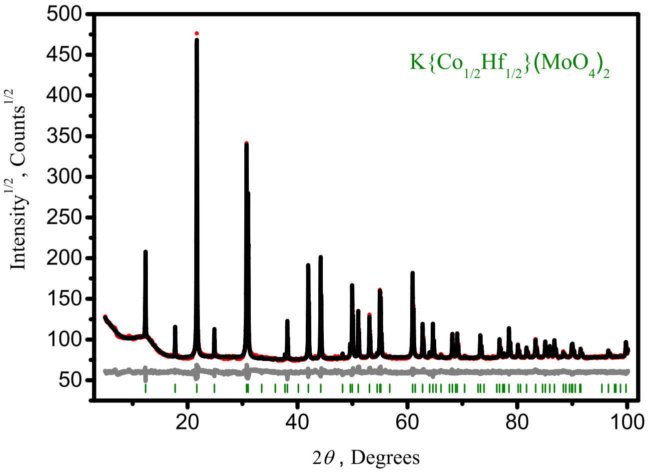

Fig. (1). Difference Rietveld plot of $KCo_{1/2}Hf_{1/2}(MoO_4)_2$.

We used fractional coordinates of $K(Mg_{0.5}Zr_{0.5})(MoO_4)_2$ in our initial structural model ($P\bar{3}m1$) [32]. The peak shapes were described using the Pearson VII function with a correction for sample texture along the *001* direction applied using the March-Dollase function.

The refinement process involved the stepwise introduction of refinable parameters, with simultaneous graphical modeling of the background.

The final refinement demonstrated stability, yielding low residual R factors. The crystallographic data for $KCo_{1/2}Hf_{1/2}(MoO_4)_2$ were deposited with the Cambridge Crystallographic Data Centre (CSD 2393645). The data are accessible on the CCDC website (www.ccdc.cam.ac.uk/data_request/cif).

The $KCo_{1/2}Hf_{1/2}(MoO_4)_2$ structure exhibits a layered crystal structure. Two distinct layers are oriented perpendicular to the *c*-axis: the first layer comprises $(Co/Hf)O_6$ octahedra, while the second consists of KO_{12}-icosahedra and MoO_4-tetrahedra, which are connected through shared oxygen edges (Fig. **2**).

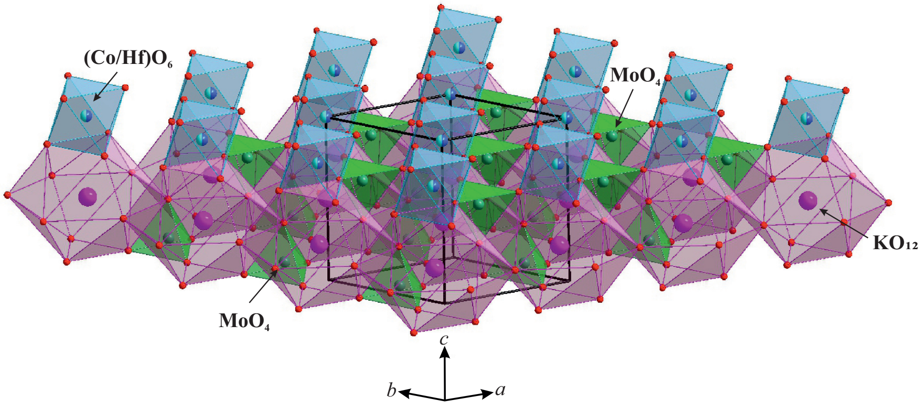

Fig. (2). The crystal structure of $KCo_{1/2}Hf_{1/2}(MoO_4)_2$.

3.2. ATR-IR Spectrum

The IR spectra of complex molybdates contain bands characteristic of vibrations of the tetrahedral MoO_4-groups. Usually, bands corresponding to stretching (980–700 cm-1) and bending modes (410–300 cm-1) of Mo–O bonds are observed [33]. The experimental IR spectra encompass only the stretching vibrational modes of the MoO_4 tetrahedra. The IR spectrum of the compound (ν_1 = 899 cm^{-1}; 862 cm^{-1}; 829cm^{-1}; ν_3 = 727cm^{-1}) confirmed the presence of MoO_4–tetrahedra and exhibited a strong similarity to the spectrum of the isostructural compound $KMg_{1/2}Zr_{1/2}(MoO_4)_2$ [30] with isolated MoO_4 tetrahedra (Fig. **3**).

3.3. Thermal Properties

The DSC curves recorded from $KCo_{1/2}Hf_{1/2}(MoO_4)_2$ are shown in (Fig. **4**). Upon heating the sample, two endothermic signals were observed at 490°C and 699°C. The endothermic peak at 699°C indicated the melting point of $KCo_{1/2}Hf_{1/2}(MoO_4)_2$. No weight loss was observed on the TG curve.

The Rietveld-refined XRD patterns of $KCo_{1/2}Hf_{1/2}(MoO_4)_2$ after annealing at 750°C indicated its partial decomposition, leading to the formation of $CoMoO_4$, $K_2Mo_3O_{10}$, $K_2Co_2(MoO_4)_3$, and HfO_2.

To further investigate the endothermic effect observed at 490°C, the sample was analyzed in a “heating-cooling” mode within the temperature range of 200–650°C. During cooling, $KCo_{1/2}Hf_{1/2}(MoO_4)_2$ exhibited an exothermic effect at 473°C, with a hysteresis of 17°C. The characteristic signal within the 473–490°C range indicated the presence of a reversible phase transition (type I) in $KCo_{1/2}Hf_{1/2}(MoO_4)_2$ (Fig. **4**).

The temperature dependences of the lattice parameters of $KCo_{1/2}Hf_{1/2}(MoO_4)_2$, resulting from the HT-PXRD experiments, are presented in Fig. (**5** and Table **4**).

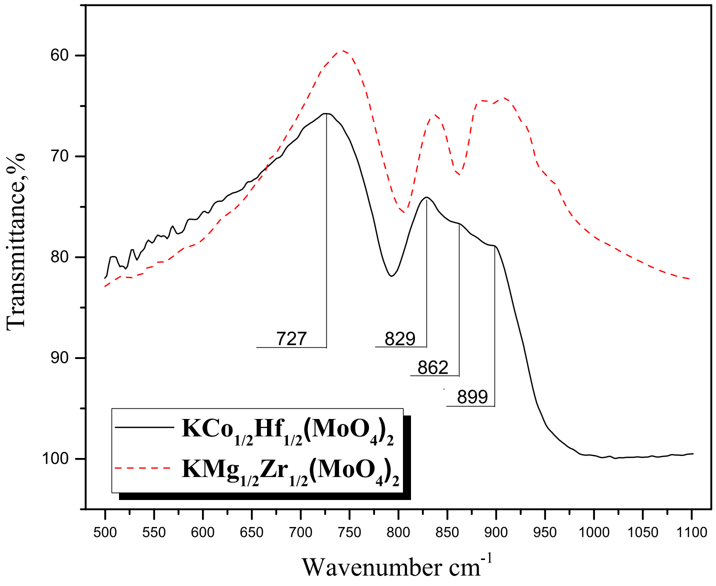

Fig. (3). IR spectra of $KCo_{1/2}Hf_{1/2}(MoO_4)_2$ и $KMg_{1/2}Zr_{1/2}(MoO_4)_2$ [30].

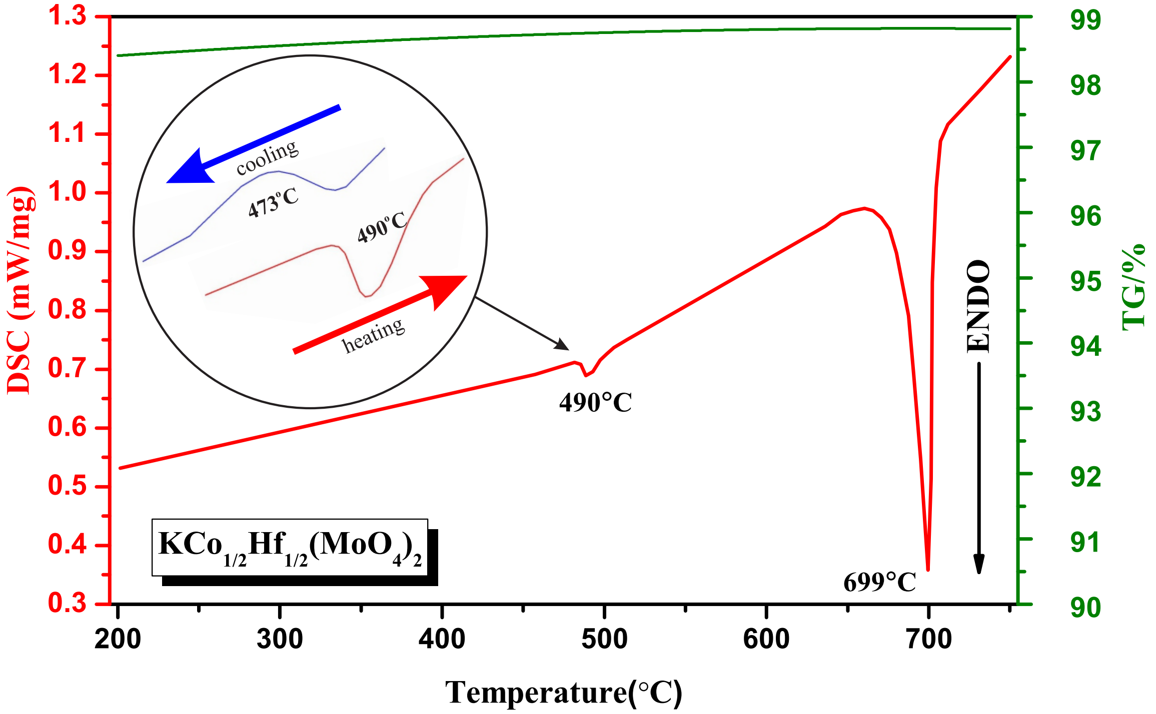

Fig. (4). TG and DSC measurements of $KCo_{1/2}Hf_{1/2}(MoO_4)_2$.

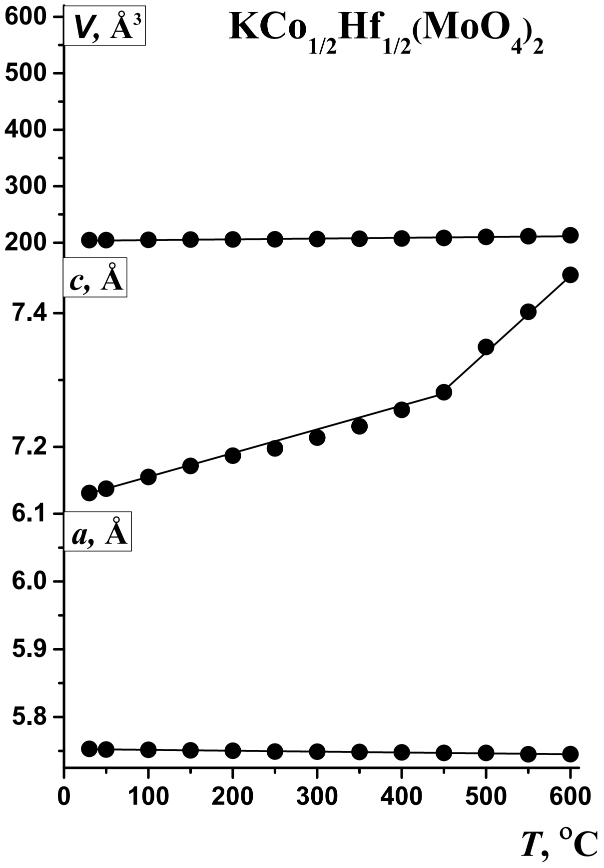

Fig. (5). The dependence of the lattice parameters of $KCo_{1/2}Hf_{1/2}(MoO_4)_2$ on temperature.

Table 4. The unit cell parameters of $KCo_{1/2}Hf_{1/2}(MoO_4)_2$.

T°C	*a*, Å	*c*, Å	*V*, Å^3
30.0	5.7528(7)	7.131(1)	204.38(6)
50.0	5.7521(3)	7.1374(7)	204.51(3)
100.0	5.7517(3)	7.1550(7)	204.99(3)
150.0	5.7507(3)	7.1716(7)	205.39(3)
200.0	5.7501(3)	7.1869(7)	205.79(3)
250.0	5.7490(3)	7.1977(7)	206.02(3)
300.0	5.7489(3)	7.2140(7)	206.48(3)
350.0	5.7484(3)	7.2308(8)	206.92(3)
400.0	5.7478(4)	7.2553(8)	207.58(4)
450.0	5.7470(4)	7.2817(8)	208.28(3)
500.0	5.7469(4)	7.3494(7)	210.21(3)
550.0	5.7451(3)	7.4021(6)	211.58(3)
600.0	5.7452(4)	7.4574(7)	213.17(3)

The decrease in the *a*-parameter value is fairly linear over the entire temperature range, while the increase in the *c*-parameter can be described by two linear segments before and after 450°C. Thus, the point of curve inflection was observed on the temperature dependence curve of the c parameter around 450-500°C (which corresponds to the DSC data), followed by a more pronounced increase in this parameter. All reflections on high-temperature X-ray diffraction patterns in the entire studied temperature range are indicated in the same space group; no new peaks were detected, which indicates that the first-order phase transition is not accompanied by a change in the structure. The most likely cause of the phase transition is a change in the electronic structure of the Co^{2+} ion. The transition from the low-spin state to the high-spin state is accompanied by a sharp increase in the ionic radius from 0.79 to 0.885 A for the Co^{2+} ion with C.N. = 6 [31]. Such a transition was observed for the compound Co_3BO_5 [34]. The temperature-dependent variations of the lattice parameters were approximated using first-order polynomial functions (Table **5**).

The coefficient of thermal expansion (CTE) calculated through the linear approximation of the temperature dependencies of the lattice parameters is shown in Table **6**, with cross-sections of the CTE illustrated in Fig. (**6**). The thermal expansion of $KCo_{1/2}Hf_{1/2}(MoO_4)_2$ is notably anisotropic, with the greatest expansion observed along the *c*-axis.

The coefficient of thermal expansion (CTE) α_c was 47×10^{-6} °C^{-1} up to 450°C and 156×10^{-6} °C^{-1}, while α_a remained negative at -2.3×10^{-6} °C^{-1} throughout the investigated temperature range. Despite this, no reduction in cell volume was observed. The values of α_V for $KCo_{1/2}Hf_{1/2}(MoO_4)_2$ were 43×10^{-6} °C^{-1} at room temperature and 148×10^{-6} °C^{-1} at 600°C. These values are close to those calculated for the isostructural analogue $KMg_{0.5}Zr_{0.5}(MoO_4)_2$ (α_V = 160×10^{-6} °C^{-1} at 500°C [30]).

The observed 2D negative thermal expansion in the *ab* plane is likely attributable to the thermal motion of the oxygen atom O2 (Wyckoff position 6i), as it is the only atom with the necessary degree of freedom. It is expected that, namely, the bond Co–O2 is the most “flexible”, that is, it has more freedom for a change. Thus, the unit cell expansion along the crystallographic c-axis can be attributed to an increase in the value of Co–O2 bond length.

3.3.1. Electrical Conductivity

The electrophysical properties of the examined ternary molybdate were also characterized. The temperature dependence of conductivity (in a heating-cooling cycle) at various frequencies and the impedance plot, which is typical for ionic conductors, are presented in Fig. (**7**).

Conductivity monotonically increased with rising temperature (100–450°C) from 10^{-9} to 10^{-6} S/cm. A subsequent sharp increase in conductivity was observed, reaching a value of $0.42\cdot10^{-3}$ S/cm (570°C) with an activation energy E_a = 0.8 eV. A deviation from linearity in the temperature dependence of conductivity was observed during both heating and cooling, specifically at 510°C and 500°C, respectively. These values correlated with the temperature of the endothermic effect detected in the DSC curve (Fig. **4**), indicating a first-order phase transition, which was further confirmed by the presence of thermal hysteresis (Fig. **7**). The pattern of the temperature dependence of conductivity is similar to that of the isostructural molybdate $KMg_{0.5}Zr_{0.5}(MoO_4)_2$. Theoretical evaluation of the energy barriers of transport based on the bond valence sum maps (BVS) showed that its structure mainly realizes two-dimensional oxygen transport [30]. It is assumed that in $KCo_{1/2}Hf_{1/2}(MoO_4)_{2,}$ the most probable charge carrier is also oxygen ions, which requires further research.

Table 5. Temperature dependencies of the lattice parameters approximated by linear polynomial functions a_0 + a_1 × $10^{-3}t$.

Cell	T_1, °C	T_2, °C	a_0	a_1	R^2
a	30	600	5.7528(2)	-0.0130(5)	1.000
c	30	450	7.119(3)	0.34(1)	0.990
c	450	600	6.78(3)	1.14(5)	0.996
V	30	600	203.0(5)	14(1)	1.000

Table 6. Thermal expansion coefficients of $KCo_{1/2}Hf_{1/2}(MoO_4)_2$ (×10^{-6} °C^{-1}).

T, °C	α_a	α_c	α_V
30	-2.26(9)	47(2)	43(7)
50	-2.26(9)	47(2)	43(7)
100	-2.26(9)	47(2)	43(7)
150	-2.26(9)	47(2)	43(7)
200	-2.26(9)	47(2)	42(7)
250	-2.26(9)	47(2)	42(7)
300	-2.26(9)	47(2)	42(7)
350	-2.26(9)	47(2)	42(7)
400	-2.26(9)	47(2)	42(7)
450	-2.26(9)	46(2)	42(7)
500	-2.26(9)	155(7)	151(7)
550	-2.26(9)	154(7)	150(7)
600	-2.27(9)	153(6)	148(7)

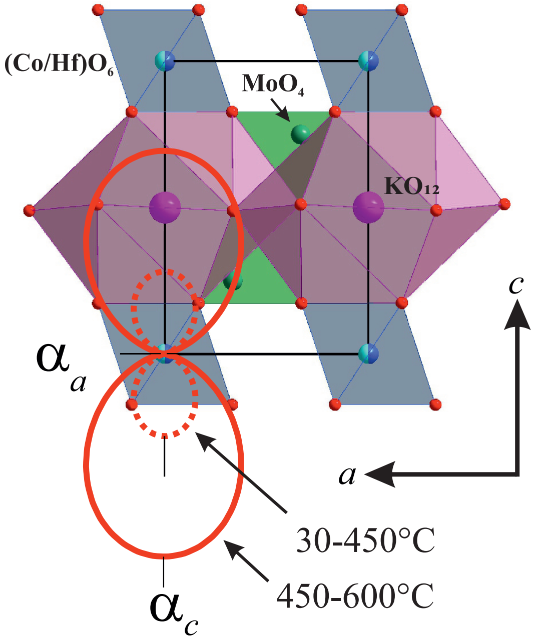

Fig. (6). Projection of the $KCo_{1/2}Hf_{1/2}(MoO_4)_2$ structure on the *ac* plane, mapped to the thermal expansion tensor cross-section.

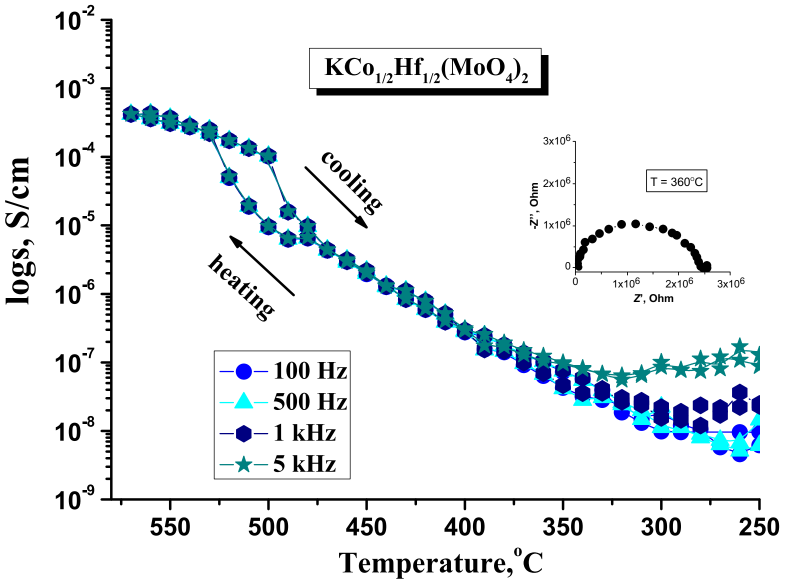

Fig. (7). Temperature dependencies of electrical conductivity for $KCo_{1/2}Hf_{1/2}(MoO_4)_2$.

CONCLUSION

Ternary molybdate $KCo_{1/2}Hf_{1/2}(MoO_4)_2$ was synthesized *via* a ceramic route. Its structure was refined by the Rietveld method, with initial parameters based on literature data for the single crystal $KMg_{0.5}Zr_{0.5}(MoO_4)_2$ sample [32]. The compound studied was crystallized in the trigonal space group *P*3-*m*1. The experimental IR spectrum had characteristic lines of the MoO_4 tetrahedra stretching modes, thus confirming the coordination of the Mo atoms in the refined structure. Differential scanning calorimetry (DSC) results demonstrated that $KCo_{1/2}Hf_{1/2}(MoO_4)_2$ melted at 699°C with decomposition. In this study, we investigated the ionic conductivity properties of $KCo_{1/2}Hf_{1/2}(MoO_4)_2$, which reached a conductivity value of $0.42 \cdot 10^{-3}$ S/cm (570°C) with an activation energy E_a = 0.8 eV. Thermal deformations of $KCo_{1/2}Hf_{1/2}(MoO_4)_2$ were investigated using HT-XRD. The observed 2D negative thermal expansion in the *ab* plane did not lead to a reduction in the cell volume. Therefore, the studied ternary molybdate $KCo_{1/2}Hf_{1/2}(MoO_4)_2$ ($\alpha_V = 148 \times 10^{-6}$ °C^{-1} at 600°C) can be categorized as a high-expansion material [35].

AUTHORS' CONTRIBUTIONS

It is hereby acknowledged that all authors have accepted responsibility for the manuscript's content and consented to its submission. They have meticulously reviewed all results and unanimously approved the final version of the manuscript.

LIST OF ABBREVIATIONS

NTE = Negative Thermal Expansion

HT-PXRD = High-temperature Powder X-ray Diffraction

CTE = Coefficient of Thermal Expansion

CONSENT FOR PUBLICATION

Not applicable.

AVAILABILITY OF DATA AND MATERIALS

The data and supportive information are available within the article.

FUNDING

This work was funded by the Russian Science Foundation (grant 23-29-00327), Russia.

CONFLICT OF INTEREST

The authors declare no conflict of interest, financial or otherwise.

ACKNOWLEDGEMENTS

The authors would like to acknowledge the resources of the Research Equipment Sharing Center of BINM SB RAS (Ulan-Ude, Russia), which were used to carry out x-ray phase analysis, high-temperature x-ray diffraction, infrared spectroscopy, and conductivity measurements.

REFERENCES

[1] S.F. Solodovnikov, O.A. Gulyaeva, A.A. Savina, V.N. Yudin, A.L. Buzlukov, Z.A. Solodovnikova, E.S. Zolotova, T.S. Spiridonova, E.G. Khaikina, S.Y. Stefanovich, N.I. Medvedeva, Y.V. Baklanova, and T.A. Denisova, "Molybdates and tungstates of the alluaudite family: Crystal chemistry, composition, and ionic mobility", *J. Struct. Chem.,* vol. 63, no. 7, pp. 1101-1133, 2022. [http://dx.doi.org/10.1134/S0022476622070071]

[2] A.L. Buzlukov, D.S. Fedorov, A.V. Serdtsev, I.Y. Kotova, A.P. Tyutyunnik, D.V. Korona, Y.V. Baklanova, V.V. Ogloblichev, N.M. Kozhevnikova, T.A. Denisova, and N.I. Medvedeva, "Ion mobility in triple sodium molybdates and tungstates with a NASICON structure", *J. Exp. Theor. Phys.,* vol. 134, no. 1, pp. 42-50, 2022. [http://dx.doi.org/10.1134/S1063776122010071]

[3] V.G. Grossman, M.S. Molokeev, B.G. Bazarov, and J.G. Bazarova, "Potassium and thallium conductors with a trigonal structure in the M2MoO4–Cr2(MoO4)3–Hf(MoO4)2 (M = K, Tl) systems: Synthesis, structure, and ionic conductivity", *J. Alloys Compd.,* vol. 873, p. 159828, 2021. [http://dx.doi.org/10.1016/j.jallcom.2021.159828]

[4] T.S. Spiridonova, S.F. Solodovnikov, A.A. Savina, Y.M. Kadyrova, Z.A. Solodovnikova, V.N. Yudin, S.Y. Stefanovich, and E.G. Khaikina, "New triple molybdate Rb 2 AgIn(MoO 4) 3 : Synthesis, framework crystal structure and ion-transport behaviour", *Acta Crystallogr. C Struct. Chem.,* vol. 74, no. 12, pp. 1603-1609, 2018. [http://dx.doi.org/10.1107/S2053229618014717] [PMID: 30516143]

[5] O.D. Chimitova, B.G. Bazarov, J.G. Bazarova, V.V. Atuchin, R. Azmi, A.E. Sarapulova, D. Mikhailova, G. Balachandran, A. Fiedler, U. Geckle, Y. Prots, A.C. Komarek, T.A. Gavrilova, I.P. Prosvirin, Y. Yang, Z. Lin, M. Knapp, and H. Ehrenberg, "The crystal growth and properties of novel magnetic double molybdate RbFe 5 (MoO 4) 7 with mixed Fe 3+ /Fe 2+ states and 1D negative thermal expansion", *CrystEngComm,* vol. 23, no. 18, pp. 3297-3307, 2021. [http://dx.doi.org/10.1039/D1CE00118C]

[6] W.B. Nasr, and A.B. Rhaiem, "Ferroelectric properties and alternative current conduction mechanisms of lithium rubidium molybdate", *Ionics,* vol. 25, no. 8, pp. 4003-4012, 2019. [http://dx.doi.org/10.1007/s11581-019-02921-w]

[7] R. Nasri, T. Larbi, M. Amlouk, and M.F. Zid, "Investigation of the physical properties of K2Co2(MoO4)3 for photocatalytic application", *J. Mater. Sci. Mater. Electron.,* vol. 29, no. 21, pp. 18372-18379, 2018. [http://dx.doi.org/10.1007/s10854-018-9951-x]

[8] B. Binish, M. Durairaj, and T.C. Girisun, "Engineering the nonlinear optical properties of barium molybdate by doping Sn4+ ions for optical limiting device applications", *Ceram. Int.,* vol. 49, no. 11, pp. 17629-17638, 2023. [http://dx.doi.org/10.1016/j.ceramint.2023.02.129]

[9] D. Stefańska, A. Kabański, M. Adaszyński, M. Ptak, R. Lisiecki, N. Starościk, and J. Hanuza, "Broadband near-infrared luminescence properties of Sc2(MoO4)3:Cr3+ molybdates", *Spectrochim. Acta A Mol. Biomol. Spectrosc.,* vol. 296, p. 122699, 2023. [http://dx.doi.org/10.1016/j.saa.2023.122699] [PMID: 37023656]

[10] H. Ren, H. Li, Y. Zou, H. Deng, Z. Peng, T. Ma, and S. Ding, "Growth and properties of Pr3+-doped NaGd(MoO4)2 single crystal: A promising InGaN laser-diode pumped orange-red laser crystal", *J. Lumin.,* vol. 249, p. 119034, 2022. [http://dx.doi.org/10.1016/j.jlumin.2022.119034]

[11] J. Wang, L. Luo, B. Huang, J. He, W. Zhang, W. Zhao, and J. Wang, "The preparation and optical properties of novel LiLa(MoO4)2:Sm3+,Eu3+ red phosphor", *Materials,* vol. 11, no. 2, p. 297, 2018. [http://dx.doi.org/10.3390/ma11020297] [PMID: 29443910]

[12] D. Spassky, A. Vasil'ev, M.U. Jamal, V.A. Morozov, B.I. Lazoryak, B.S. Redkin, K. Chernenko, and V. Nagirnyi, "Temperature dependent energy transfer to Eu 3+ emission centres in K 5 Eu(MoO 4) 4 crystals", *CrystEngComm,* vol. 26, no. 8, pp. 1106-1116, 2024. [http://dx.doi.org/10.1039/D3CE01201H]

[13] G.D. Tsyrenova, E.T. Pavlova, S.F. Solodovnikov, N.N. Popova, T.Y. Kardash, S.Y. Stefanovich, I.A. Gudkova, Z.A. Solodovnikova, and B.I. Lazoryak, "New ferroelastic K2Sr(MoO4)2: Synthesis, phase transitions, crystal and domain structures, ionic conductivity", *J. Solid State Chem.,* vol. 237, pp. 64-71, 2016. [http://dx.doi.org/10.1016/j.jssc.2016.01.011]

[14] M. Liu, Y. Zhang, T. Zou, V.O. Garlea, T. Charlton, Y. Wang, F. Liu, Y. Xie, X. Li, L. Yang, B. Li, X. Wang, S. Dong, and J.M. Liu, "Antiferromagnetism of double molybdate LiFe(MoO4)2", *Inorg. Chem.,* vol. 59, no. 12, pp. 8127-8133, 2020. [http://dx.doi.org/10.1021/acs.inorgchem.0c00432] [PMID: 32484663]

[15] P. Loiko, A. Pavlyuk, S. Slimi, R.M. Solé, E. Ben Salem, E. Dunina, A. Kornienko, P. Camy, U. Griebner, V. Petrov, F. Díaz, M. Aguiló, and X. Mateos, "Growth, spectroscopy and laser operation of monoclinic Nd:CsGd(MoO4)2 crystal with a layered structure", *J. Lumin.,* vol. 231, p. 117793, 2021. [http://dx.doi.org/10.1016/j.jlumin.2020.117793]

[16] H. Ishizaki, Y. Sakai, T. Nishikubo, Z. Pan, K. Oka, H. Yamamoto, and M. Azuma, "Negative thermal expansion in lead-free lasubstituted Bi0.5Na0.5VO3", *Chem. Mater.,* vol. 32, no. 11, pp. 4832-4837, 2020. [http://dx.doi.org/10.1021/acs.chemmater.0c01709]

[17] S. Deng, Y. Sun, H. Wu, Q. Huang, J. Yan, K. Shi, M.I. Malik, H. Lu, L. Wang, R. Huang, L. Li, and C. Wang, "Invar-like behavior of antiperovskite Mn3+xNi1−xN compounds", *Chem. Mater.,* vol. 27, no. 7, pp. 2495-2501, 2015. [http://dx.doi.org/10.1021/cm504702m]

[18] H. Zou, X. Yang, B. Chen, Y. Du, B. Ren, X. Sun, X. Qiao, Q. Zhang, and F. Wang, "Thermal enhancement of upconversion by negative lattice expansion in orthorhombic Yb2W3O12", *Angew. Chem. Int. Ed.,* vol. 58, no. 48, pp. 17255-17259, 2019. [http://dx.doi.org/10.1002/anie.201910277] [PMID: 31523889]

[19] Q. Gao, J. Wang, A. Sanson, Q. Sun, E. Liang, X. Xing, and J. Chen, "Discovering large isotropic negative thermal expansion in framework compound AgB(CN)4via the concept of average atomic volume", *J. Am. Chem. Soc.,* vol. 142, no. 15, pp. 6935-6939, 2020. [http://dx.doi.org/10.1021/jacs.0c02188] [PMID: 32233466]

[20] Y. Song, J. Chen, X. Liu, C. Wang, J. Zhang, H. Liu, H. Zhu, L. Hu, K. Lin, S. Zhang, and X. Xing, "Zero thermal expansion in magnetic and metallic Tb(Co,Fe)2 intermetallic compounds", *J. Am. Chem. Soc.,* vol. 140, no. 2, pp. 602-605, 2018. [http://dx.doi.org/10.1021/jacs.7b12235] [PMID: 29292996]

[21] M. Azuma, W. Chen, H. Seki, M. Czapski, S. Olga, K. Oka, M. Mizumaki, T. Watanuki, N. Ishimatsu, N. Kawamura, S. Ishiwata, M.G. Tucker, Y. Shimakawa, and J.P. Attfield, "Colossal negative thermal expansion in BiNiO3 induced by intermetallic charge transfer", *Nat. Commun.,* vol. 2, no. 1, p. 347, 2011. [http://dx.doi.org/10.1038/ncomms1361] [PMID: 21673668]

[22] J. Chen, Q. Gao, A. Sanson, X. Jiang, Q. Huang, A. Carnera, C.G. Rodriguez, L. Olivi, L. Wang, L. Hu, K. Lin, Y. Ren, Z. Lin, C. Wang, L. Gu, J. Deng, J.P. Attfield, and X. Xing, "Tunable thermal expansion in framework materials through redox intercalation", *Nat. Commun.,* vol. 8, no. 1, p. 14441, 2017. [http://dx.doi.org/10.1038/ncomms14441] [PMID: 28181576]

[23] T. Yang, K. Lin, Q. Li, Y. Wang, L. Gu, N. Wang, J. Deng, J. Chen, and X. Xing, "Evidence of the enhanced negative thermal expansion in (1 − x)PbTiO 3 - x Bi(Zn 2/3 Ta 1/3)O 3", *Inorg. Chem. Front.,* vol. 7, no. 5, pp. 1284-1288, 2020. [http://dx.doi.org/10.1039/C9QI01694E]

[24] Y. Song, Q. Sun, M. Xu, J. Zhang, Y. Hao, Y. Qiao, S. Zhang, Q. Huang, X. Xing, and J. Chen, "Negative thermal expansion in (Sc,Ti)Fe 2 induced by an unconventional magnetovolume effect", *Mater. Horiz.,* vol. 7, no. 1, pp. 275-281, 2020. [http://dx.doi.org/10.1039/C9MH01025D]

[25] Q. Li, H. Zhu, L. Hu, J. Chen, and X. Xing, "Negative thermal expansion in nanosolids", *Acc. Chem. Res.,* vol. 52, no. 9, pp. 2694-2702, 2019. [http://dx.doi.org/10.1021/acs.accounts.9b00260] [PMID: 31393697]

[26] E. Kovtunets, Y. Tushinova, B. Bazarov, J. Bazarova, A. Logvinova, and T. Spiridonova, "Ho2Zr(MoO4)5 — A novel double molybdate with negative thermal expansion", *Solid State Sci.,* vol. 150, p. 107482, 2024. [http://dx.doi.org/10.1016/j.solidstatesciences.2024.107482]

[27] J. Chen, L. Hu, J. Deng, and X. Xing, "Negative thermal expansion in functional materials: controllable thermal expansion by chemical modifications", *Chem. Soc. Rev.,* vol. 44, no. 11, pp. 3522-3567, 2015. [http://dx.doi.org/10.1039/C4CS00461B] [PMID: 25864730]

[28] A.A. Coelho, "TOPAS and TOPAS-Academic : An optimization program integrating computer algebra and crystallographic objects written in C++", *J. Appl. Cryst.,* vol. 51, no. 1, pp.

210-218, 2018.
[http://dx.doi.org/10.1107/S1600576718000183]

[29] R.S. Bubnova, V.A. Firsova, and S.K. Filatov, "Software for determining the thermal expansion tensor and the graphic representation of its characteristic surface (theta to tensor-TTT)", *Glass Phys. Chem.,* vol. 39, no. 3, pp. 347-350, 2013.
[http://dx.doi.org/10.1134/S108765961303005X]

[30] E. Kovtunets, Y. Tushinova, B. Bazarov, J. Bazarova, A. Logvinova, and T. Spiridonova, "A glaserite-like ternary molybdate K(Mg0.5Zr0.5)(MoO4)2: Synthesis, thermal expansion, and ionic conductivity", *Solid State Sci.,* vol. 151, p. 107528, 2024.
[http://dx.doi.org/10.1016/j.solidstatesciences.2024.107528]

[31] R.D. Shannon, "Revised effective ionic radii and systematic studies of interatomic distances in halides and chalcogenides", *Acta Crystallogr. A,* vol. 32, no. 5, pp. 751-767, 1976.
[http://dx.doi.org/10.1107/S0567739476001551]

[32] R.F. Klevtsova, Z.G. Bazarova, L.A. Glinskaya, V.I. Alekseev, S.I. Arkhincheeva, B.G. Bazarov, and P.V. Klevtsov, "Crystal structure investigation of ternary molybdate K(Mg0.5Zr0.5).(MoO4)2", *J. Struct. Chem.,* vol. 36, no. 5, pp. 809-812, 1995.
[http://dx.doi.org/10.1007/BF02579673]

[33] V.V. Fomichev, M.E. Poloznikova, and O.I. Kondratov, "Structural features and spectroscopic and energy characteristics of alkali metal molybdates and tungstates", *Russ. Chem. Rev.,* vol. 61, no. 9, pp. 877-888, 1992.
[http://dx.doi.org/10.1070/RC1992v061n09ABEH001004]

[34] N. Kazak, A. Arauzo, J. Bartolomé, M. Molokeev, V. Dudnikov, L. Solovyov, A. Borus, and S. Ovchinnikov, "Anisotropic thermal expansion and electronic transitions in the Co 3 BO 5 ludwigite", *Dalton Trans.,* vol. 51, no. 16, pp. 6345-6357, 2022.
[http://dx.doi.org/10.1039/D2DT00270A] [PMID: 35383815]

[35] V.I. Pet’kov, A.S. Shipilov, and M.V. Sukhanov, "Thermal expansion of MZr2(AsO4)3 and MZr2(TO4) x (PO4)3–x (M = Li, Na, K, Rb, Cs; T = As, V)", *Inorg. Mater.,* vol. 51, no. 11, pp. 1079-1085, 2015.
[http://dx.doi.org/10.1134/S002016851510012X]